Improvement of lithium adsorption capacity by optimising the parameters affecting synthesised ion sieves

Saeed Zandevakili[1], Mohammad Ranjbar[2], Maryam Ehteshamzadeh[3]

[1]*Department of Mining Engineering, Shahid Bahonar University, Kerman, P.O. Box 76169-133, Iran*
[2]*Mineral Industries Research Centre, Shahid Bahonar University, Kerman, P.O. Box 76169-133, Iran*
[3]*Department of Material Engineering, Shahid Bahonar University, Kerman, P.O. Box 76169-133, Iran*
E-mail: saeedzand2001@yahoo.com

Published in Micro & Nano Letters; Received on 13th June 2014; Revised on 15th October 2014; Accepted on 17th October 2014

Recent study has shown that the spinel type of MnO_2 nanoparticles have a required capacity for lithium extraction from liquid resources. The low lithium adsorption capacity of synthesised ion sieves was found to be an important limiting parameter for their use in industrial applications. Therefore, increasing the uptake capacity of different ion sieves by studying the effect of six effective parameters, involving lithium salt compound, manganese salt compound, oxidising reagent, calcination temperature, heating time and Li/Mn mol ratio, on the synthesised ion sieves was investigated. Hence, in this reported work, a specific approach based on the $L_9(3^4)$ Taguchi orthogonal array was employed to evaluate these parameters and to optimise them in two separate stages. Also, the relative importance of each factor was determined using analysis of variance. Although, all mentioned parameters had a significant effect on lithium uptake capacity, the oxidising reagent and the lithium salt compound were the most effective factors. Also, an appropriate ion sieve with a lithium adsorption capacity of more than 9 mmol g^{-1} was synthesised for the first time.

1. Introduction: Certain inorganic adsorbents with extremely high selectivity for lithium ions are called lithium ion sieves. Owing to their noticeable properties such as low toxicity, low cost, high chemical stability and high Li^+ adsorption capacity, lithium ion sieves are suitable for the recovery of lithium from salt lake brine and seawater [1–4].

Manganese oxides derived from spinel lithium manganese oxides after topotactical extraction of lithium from the spinel framework are one of the typical lithium ion sieves and are the most widely studied. This nanostructure material has been used to adsorb Li^+ from lithium solutions, and has been shown to satisfy adsorption performances [5–7]. Over the past 20 years, numerous studies have been conducted for synthesising ion sieves with high Li^+ adsorption capacity. In 1990, an alumina–magnesia mixed oxide gel with the uptake capacity of 0.014 mmol g^{-1} lithium from seawater was synthesised by Kaneko [8]. In 2000, Chitrakar *et al.* synthesised the spinel manganese antimony oxide with the lithium adsorption capacity of 2 mmol g^{-1} [9]. Subsequently, in 2000, $MnO_2{\cdot}0.5H_2O$ was produced as a new ion sieve with an adsorption capacity of more than 5 mmol g^{-1} [10]. Stronger ion sieves with an adsorption capacity of 5.7 mmol g^{-1} were manufactured by optimising the calcination temperature and Li/Mn mole ratio [11]. In 2002, a λ-MnO_2 ion sieve with an adsorption capacity of 3.8 mmol g^{-1} was synthesised by Lei *et al.* using the solid phase reaction of Li_2CO_3 and Mn_2O_3 at 850°C and acid treatment of the synthesised precursor in column [12]. In 2006, Wang *et al.* synthesised two different ion sieves with the maximum adsorption capacity of 3.17 mmol g^{-1} through the solid phase reaction of a mixture of $MnCO_3$ and two different sources of lithium including Li_2CO_3 and LiOH in different molar ratios of Li/Mn at 450°C, followed by acid treatment of the precursor [13]. In 2007, Zhang *et al.* produced four different ion sieves using $MnSO_4{\cdot}H_2O$ in the presence of different oxidising agents including $(NH_4)_2S_2O_8$, $(NH_4)_2SO_4$ and $LiOH{\cdot}H_2O$ as the lithium resource. The maximum adsorption capacity at optimised temperatures attained was 4.2 mmol g^{-1} [14]. Again, in 2009, Zhang *et al.* synthesised a new ion sieve with an adsorption capacity of more than 6.5 mmol g^{-1} with some changes in the type of lithium salt compounds, calcination temperature and time [15]. Using $MnCl_2{\cdot}4H_2O$ in the presence of LiOH, H_2O_2 and acid treatment of the resulting precursor led to the synthesis of a new ion sieve with an adsorption capacity of more than 5.33 mmol g^{-1} [16]. Afterwards, in 2010, Tian *et al.* manufactured a new manganese/magnesium ion sieve with the adsorption capacity close to 5.38 mmol g^{-1} in the presence of $MnCl_2{\cdot}4H_2O$, $Mg(NO_3)_2{\cdot}6H_2O$, LiOH and H_2O_2 as the oxidising agent [17]. Moreover, direct synthesis of a $LiMn_2O_4$ spinel was investigated by Zhang *et al.* in 2010, and an ion sieve with the maximum absorption capacity of 3.42 mmol g^{-1} was achieved [18]. In the same year, Özgür synthesised a new ion sieve by ultrasonic spray pyrolysis and the ion sieve capacity reached 5.57 mmol g^{-1} in the best condition [19]. Simultaneously, Ma *et al.* investigated the stabilisation of $LiM_xMn_{2-x}O_4$ (M:Ni, Al, Ti $0 \le x \le 1$) and the uptake properties of their ion sieves. The results showed that the maximum adsorption capacity reached 1.53, 2.93 and 1.35 mmol g^{-1} by applying ion sieves synthesised by Ti, Al and Ni, respectively [20]. The strongest ion sieve synthesised by Sun *et al.* in the presence of $LiNO_3$ increased the capacity to 6.67 mmol g^{-1} [21]. Although the influence of some controlling parameters such as Li/Mn mole ratio, calcination temperature or heating time on lithium ion sieve capacity has been investigated by different researchers, there is no systematic study on these parameters and their effect. Also, the effects of some parameters like oxidising reagent, lithium and manganese salt compound have not been compared yet.

Therefore, in this present Letter, Taguchi method, as a combination of mathematical and statistical techniques, is used to optimise the experimental parameters for increasing lithium uptake capacity. The Taguchi method not only uses fewer experiments for optimisation of the levels of various parameters, but also can determine the experimental conditions having the least variability as the optimum conditions [22–24]. In this Letter, the contribution of the six controlled factors involving manganese salt compound (Mn.S.C.), lithium salt compound (Li.S.C.), oxidising reagent (Ox.R), Li/Mn mole ratio (Mol.R.), calcinations temperature (Cal.Te) and heating time (He.Ti) on the synthesised ion sieve is investigated. In summary, synthesising a new ion sieve improved characterisation, especially in lithium uptake capacity, and the main objective of this reported work was accomplished.

© The Institution of Engineering and Technology 2015

doi: 10.1049/mnl.2014.0342

2. Experimental procedures

2.1. Synthesis of ion sieves: All chemicals used in this work were Merck reagents. A 250 millilitre mixed solution of Mn.S.C (0.33 mol l^{-1}) and Ox.R (0.33 mol l^{-1}) was added into a teflon-coated stainless autoclave and stirred vigorously at 250 r min^{-1}. After the mixed solution was maintained in air at room temperature for 2 h, the autoclave was sealed and heated at 393 K for 12 h, and then cooled naturally to room temperature. The obtained black precipitate (named as MO) was filtrated, washed completely with deionised water till the conductance of filtrate reached the same level of the deionised water and dried at 393 K for 12 h. The spinel type of lithium manganese oxide precursor (named as LMO) was prepared by wet impregnation of an aqueous solution of Li.S.C (0.5 mol l^{-1} with different designed Li/Mn mol ratios) into MO black solid. Then the mixture was heated to remove water at 393 K for 12 h in the drier and calcined at a designed temperature and a designed time in static air. The Li^+ extraction from the Li–Mn–O precursor was carried out in 0.5 mol l^{-1} HCl solution at 303 K for 48 h until the lattice Li^+ was completely extracted. The acid-treated materials were filtered, washed with deionised water and dried at 393 K for 12 h to obtain the final MnO_2 ion-sieves (named as HMO).

2.2. Design of experiments: Experimental design approaches were used to optimise the processing parameters and to study the parametric influence on responses. However, conventional experimental design methods, especially full-factorial approaches, are generally complex and do not always provide the desired results. Moreover, these methods require a large number of experiments when the number of factors increases. So far, several innovative experimental designs have therefore been suggested, of which the Taguchi approach has received much attention in recent years [24]. In the current study, six processing variables, which are assumed to be important parameters, with three levels for each, were first selected and a Taguchi experimental design based on a L_9 orthogonal array were then employed to study their effects on the lithium uptake capacity of synthesised ion sieves. To optimise the lithium uptake capacity, total experiments were conducted in two stages. Table 1 shows the selected three variables involving (Mn.S.C.), (Li.S.C.), (Mol.R.) and their three levels, along with the L_9 matrix designed in this first stage of the optimisation study. The other parameters were fixed. SO $(NH_4)_2S_2O_8$ was selected as (Ox.R) and (Cal.Te) and (He.Ti) were adjusted to 450°C and 6 h, respectively. The Taguchi $L_9(3^4)$ statistical design array which indicates the combination of factors and levels for the synthesis of ion sieves is given in Table 2.

After performing the experiments, the output variables were analysed to extract independently the main effects of the input factors. So, statistical analysis such as the analysis of mean (ANOM) and the analysis of variance (ANOVA) were performed to find the optimum levels of each controlling factor and to estimate how much the variance in lithium uptake is due to control factors or experiment error, respectively, [25, 26]. Furthermore, the percentage contribution of each factor was determined by this method [27]. Finally, confirmation tests were conducted.

Table 1 Main controlling factors and their levels (first stage of experiment)

Factor	Level		
	1	2	3
Mn.S.C	$MnSO_4{\cdot}H_2O$	$MnCl_2{\cdot}6H_2O$	$Mn(NO_3)_2{\cdot}4H_2O$
Li.S.C	LiOH	$LiNO_3$	$Li_2B_4O_7$
Mol.R	0.6	1	1.5

Table 2 Experimental condition based on Taguchi $L_9(3^4)$ array (first stage of experiment)

Experiment no.	Mn.S.C.	Li.S.C.	Mol.R.
1	$MnSO_4{\cdot}H_2O$	LiOH	0.6
2	$MnSO_4{\cdot}H_2O$	$LiNO_3$	1
3	$MnSO_4{\cdot}H_2O$	$Li_2B_4O_7$	1.5
4	$MnCl_2{\cdot}6H_2O$	LiOH	1
5	$MnCl_2{\cdot}6H_2O$	$LiNO_3$	1.5
6	$MnCl_2{\cdot}6H_2O$	$Li_2B_4O_7$	0.6
7	$Mn(NO_3)_2{\cdot}4H_2O$	LiOH	1.5
8	$Mn(NO_3)_2{\cdot}4H_2O$	$LiNO_3$	0.6
9	$Mn(NO_3)_2{\cdot}4H_2O$	$Li_2B_4O_7$	1

Table 3 Main controlling factors and their levels (second stage of experiment)

Factor	Level		
	1	2	3
Ox.R	$Na_2S_2O_8$	$(NH_4)_2S_2O_8$	$KMnO_4$
Cal.Te, °C	450	500	550
He.Ti, h	6	12	18

Table 4 Experimental condition based on Taguchi $L_9(3^4)$ array (second stage of experiment)

Experiment no.	Ox.R	Cal.Te, °C	He.Ti, h
1	$Na_2S_2O_8$	450	6
2	$Na_2S_2O_8$	500	12
3	$Na_2S_2O_8$	550	18
4	$(NH_4)_2S_2O_8$	450	12
5	$(NH_4)_2S_2O_8$	500	18
6	$(NH_4)_2S_2O_8$	550	6
7	$KMnO_4$	450	18
8	$KMnO_4$	500	6
9	$KMnO_4$	550	12

By optimising (Mn.S.C.), (Li.S.C.) and (Mol.R.) in the former experiment, the effect of three remaining controlling factors, involving (Ox.R), (Cal.Te) and (He.Ti), were investigated. Similar to the previous test, these experiments were accomplished in three levels by $L_9(3^4)$ orthogonal arrays. The optimised factors in the previous tests were selected as fixed conditions in the new tests. The process parameters and their levels for these tests are given in Table 3. Furthermore, Table 4 shows the selected L_9 orthogonal array with the assignment of parameters. It is also worth mentioning that some variables and their levels have never previously been investigated. Hence, in this Letter, not only the optimisation of operating conditions is considered, but also the synthesis of the lithium ion sieve under relatively novel conditions is studied.

In this Letter, the lithium uptake was carried out by stirring (300 r min^{-1}) 100 mg of each ion sieve in 100 ml of lithium enriched buffer solution (pH = 11) with a uniform initial Li^+ concentration of 20 mmol l^{-1} at 25°C, and the Li^+ concentration of supernatant solution was determined after 120 h by ICP. (Q_e), the amount of Li^+ adsorbed per gram of ion sieve at equilibrium (mmol g^{-1}) was also calculated according to (1), where C_e is the concentration, of metal ions at equilibrium (mmol l^{-1}), C_0 is the initial concentration of lithium ions (mmol l^{-1}), W is the weight of adsorbent (g) and V is the solution volume (ml) [15, 20]

$$Q_e = (C_0 - C_e) \cdot V/W \quad (1)$$

© The Institution of Engineering and Technology 2015

2.3. Distribution coefficient (K_d) measurements: The selectivity of Li^+ compared with other coexisting cations was carried out by stirring about 100 mg of the optimised HMO ion sieve from this research in 10 ml of enriched solution containing 17 mmol l^{-1} Li^+, Na^+, K^+ and Mg^{2+}, respectively, for 120 h at 303 K and at pH = 10. The distribution coefficient (K_d), separation factor (α_M^{Li}) and at concentration factor (C_F) were calculated according to the following equations [15]

$$K_d = (C_0 - C_e) \cdot V/(C_e \cdot W) \quad (2)$$

$$\alpha_{Me}^{Li} = K_d(Li)/K_d(Me) \quad M{:}Li, Na, K and Mg \quad (3)$$

$$C_F = Q_e(Me)/C_0(Me) \quad (4)$$

2.4. Materials characterisation: The crystalline structure of the precursor and synthesised adsorbent were determined by X-ray phase analysis (XRD, PHILIPS, X'pert MPD system, λ = 1.54 Å) with Kα Cu radiation. The morphology and average particle size of the synthesised adsorbent nanoparticles were characterised by scanning electron microscopy (SEM, Tescan Vega-II) and transmission electron microscopy (TEM, PHILIPS CM20). Inductively coupled plasma optical emission spectrometry (ICP, VARIAN OES) was used for the determination of initial and final Li^+ concentrations.

3. Results and discussion

3.1. First stage of experiment: The results of the matrix experiment which was conducted under the conditions of Table 2 are illustrated in Table 5. The lithium uptake capacity, ranges from 1.47 to 8.49 mmol g^{-1}. Table 6 shows the ANOVA for the result of nine experiments of lithium adsorption capacity. In this Table, SS, F, V and ρ% represent the sum of squares because of variation about the mean, degrees of freedom, sum of squares per degree of freedom ($V_{factor} = SS_{factor}/F$) and percentage contribution of the relative effect (SS_{factor}/SS_{total}) × 100, respectively. Subsequently, the $F_{value}(F_{factor} = V_{factor}/V_{error})$ and P_{value} were calculated. As illustrated in Table 6, F_{value} of the whole factors was greater than the extracted F_{value} of the Table for ($\alpha = 0.05$). It means that the variance of all factors is significant compared with the variance of error and all of them have a significant effect on the response. The significance of each coefficient was also determined by p_{values}, which are listed in this Table. P_{value} less than 0.05 indicate that model terms are significant.

Table 5 Results of first stage experiments

Experiment no.	Lithium adsorption, mmol g^{-1}
1	5.89
2	7.44
3	2.33
4	1.96
5	3.24
6	1.47
7	3.56
8	8.49
9	2.4

Table 6 Analysis of variance (first stage of experiment) $F(0.05, 2, 2) = 19$

	SS_{factor}	Df	V	F-value	p-value	
model	51.9	6	8.65	61.24	0.0162	significant
Mn.S.C	15.87	2	7.93	56.18	0.0175	
Li.S.C	28.4	2	14.2	100.54	0.0098	
Mol.R	7.63	2	3.82	27.02	0.0357	
error	0.28	2	0.14			
total	52.18	8				

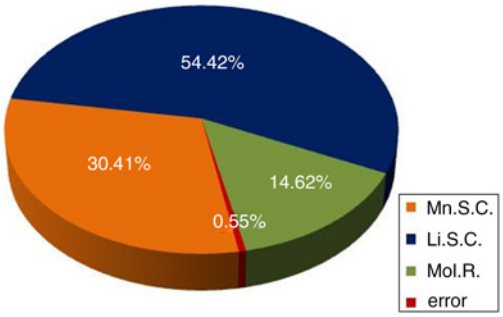

Figure 1 *Contribution of each factor on the response (first stage of experiment)*

As mentioned, the contribution of each factor to the synthesised ion sieves for lithium adsorption was determined as presented in Fig. 1. This analysis reveals that the order of factors that influence the lithium uptake are Li.S.C > Mn.S.C > Mol.R, respectively. The error variance contribution is 0.55%. In other words, the experiment in this work has 99.45% of confidence if the interaction of factors is not considered. Fig. 2 shows the effect of each parameter level on the response variable, and demonstrates that the best adsorption was obtained when Mn.S.C was set at the first and the third levels, Li.S.C at the second level, and MOL.R at the first level. Generally, in the equilibrium reaction $R\text{-}H^+ + Li^+ \Leftrightarrow R\text{-}Li^+ + H^+$ according to the Le Chatelier's principle, increasing the lithium uptake could be achieved by removing proton ions from the medium solution, which could be attained by adding OH^- ions. Raising the pH of the solution or enhancing the intrinsic acidity of the exchange sites increases lithium ion adsorption. It seems that the increase in the intrinsic acidity of the ion sieve sites could be assigned to the nucleating pH during processing. Therefore, strong acidity is advantageous for the sorption of lithium from a weak basic solution like seawater [11, 21]. Furthermore, the effect of the Mol.R factor is shown in Fig. 2. As can be seen, increase in Li/Mn mole ratio decreases the lithium uptake. This could be satisfied by generation of different amounts of the impurity phase like Mn_2O_3 and Mn_3O_4, especially when the Li/Mn mole ratio is larger than 0.7. This fact is confirmed in a previously published paper [13].

Regarding the Mn.S.C factor, the uptake of lithium ions increases in the order of $MnCl_2{\cdot}6H_2O < Mn(NO_3)_2{\cdot}4H_2O < MnSO_4{\cdot}H_2O$. In addition, concerning the Li.S.C factor, the increase in lithium

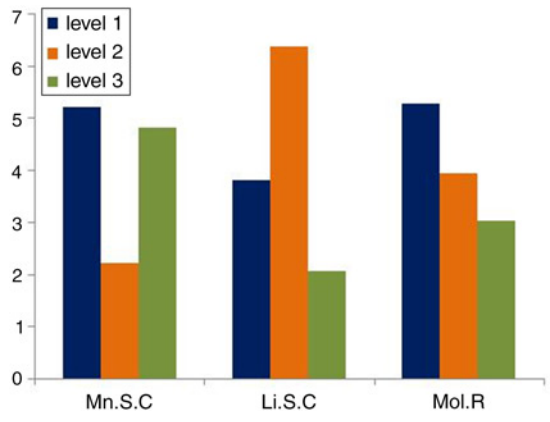

Figure 2 *Effect of each parameter level on the response variable (first stage of experiment)*

© The Institution of Engineering and Technology 2015

doi: 10.1049/mnl.2014.0342

adsorption follows the order of $Li_2B_4O_7 < LiOH < LiNO_3$ and it is the most significant factor. This reality could be satisfied by the fabrication of the strong acidity sites during the synthesis process.

Prediction of lithium uptake at optimised conditions was the last objective of the Taguchi statistical design and one of the most important goals of this research. By determination of optimised factors and their levels, the optimised lithium ion sieve will be predicted by the following equations [22, 28]

$$\overline{Y} = \frac{\sum_{i=1}^{n} y_i}{n} = 4.086 \quad (5)$$

$$Y_{Opt} = \bar{y} + (A_1 - \bar{y}) + (B_2 - \bar{y}) + (C_1 - \bar{y}) = 8.7 \quad (6)$$

In (5), $\bar{y}$ is the grand average of the responses and in (6) Y_{Opt} is the predicted surface area at the optimum condition. After prediction, a verification test should be conducted. In this step, two samples were prepared under the optimum condition ($Mn.S.C_{1and3}$, $Li.S.C_2$ and $Mol.R_1$) named 10, 11. The lithium uptake of samples 10 and 11 was measured as 7.64 and 8.56 mmol g^{-1}, respectively. Therefore, the best result formed under the optimum condition ($Mn.S.C_3$, $Li.S.C_2$ and $Mol.R_1$) and the difference between the predicted (8.7 mmol g^{-1}) and the achieved values is negligible. The low error of (1.6%) confirms the predictability of the process and the accuracy of the experimental results.

3.2. Second stage of experiment: As mentioned, these tests were conducted by applying the optimised condition from the previous tests. The whole lithium uptake with synthesised ion sieves under the conditions presented in Table 3 are listed in Table 7. Table 8 shows the results of the ANOVA. Comparing the two *F*-values of factors, the Table demonstrates that all parameters have a significant effect on the response.

The contribution of each factor on the synthesised ion sieves for lithium adsorption is shown in Fig. 3. This analysis reveals that the oxidising agent as the main factor has the greatest impact on uptake capacity. Fig. 4 shows the effect of each parameter level on the response variable and demonstrates that the best uptake capacity was obtained when all factors were set at their first levels. Then, the prediction of lithium uptake at the optimised conditions was conducted. By identifying the optimal parameters, the optimised ion sieve will be predicted by the following equations [22, 28]

$$\overline{Y} = \frac{\sum_{i=1}^{n} y_i}{n} = 5.97 \quad (7)$$

$$Y_{Opt} = \bar{y} + (A_1 - \bar{y}) + (B_1 - \bar{y}) + (C_1 - \bar{y}) = 9.11 \quad (8)$$

After prediction, a confirmation test should be conducted. In this step, a sample was prepared under the optimum condition (Ox.R_1, Cal.Te_1 and He.Ti_1) named HMO_{Final}. The lithium uptake of this sample was measured to be 9.04 mmol g^{-1}, which is the maximum among the adsorbents studied to date. Since the difference between the predicted (9.11 mmol g^{-1}) and the achieved values is negligible (0.07 mmol g^{-1}) the result is reliable.

Concerning the Cal.Te factor, the increase in lithium adsorption follows the order of 550° < 500° < 450°. The extractability of lithium from the heat-treated samples was investigated using a 0.5 M HCl solution. The Li^+ extractability reached to 99.5% for the lithium manganese oxides obtained at 450°C. However, the extractability was decreased by increasing the calcination temperature for samples obtained above 450°C, as only 88% of lithium ion could be extracted for the sample calcined at 550°C. The difference in the lithium extractability may have been because of the differences in the lithium distribution in the solid depending on the heating temperature. Regarding the He.Ti factor, the uptake of lithium ions increases in the order of 18 h < 12 h < 6 h. Therefore, it has confirmed the previous report, in which increase in calcination time decreased the lithium uptake [13]. However, an increase in heating time improves the spinel phase crystalline, but increases the content of impurities especially Mn_2O_3 and Mn_3O_4. The formation of the Mn_2O_3 impurity, with Li^+ adsorption capacity less than 1.1 mg g^{-1}, could be the primary reason for decreasing Li^+ uptake with the increase of heating time [13]. On the subject of the Ox.R factor, the uptake of lithium ions increases in the order of

Table 7 Result of second stage of experiments

Experiment no.	Lithium adsorption, mmol g^{-1}
1	9.11
2	8.63
3	7.46
4	7.23
5	6.62
6	6.31
7	2.78
8	3.44
9	2.17

Table 8 Analysis of variance (second stage of experiment) $F(0.05, 2, 2) = 19$

	SS_{factor}	df	*V*	*F*-value	*p*-value	
model	52.27	6	8.71	618.82	0.0016	significant
Ox.R	49.61	2	24.81	1762	0.0006	
Cal.TE	1.98	2	1	70.48	0.014	
He.Ti	0.67	2	0.34	23.91	0.0.04	
error	0.028	2	0.014			
total	52.3	8				

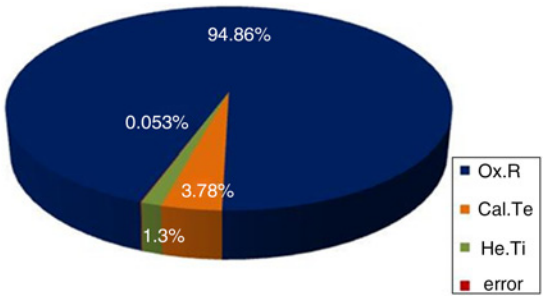

Figure 3 *Contribution of each factor on the response (second stage of experiment)*

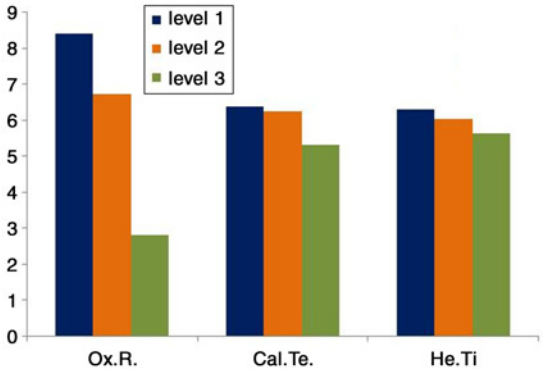

Figure 4 *Effect of parameter levels on the response variable (second stage of experiment)*

© The Institution of Engineering and Technology 2015

Table 9 Li^+ adsorption selectivity on HMO ion sieve

Me Ions	C_0 (mmol.L^{-1})	C_e	Q_e (mmol.g^{-1})	C_F ($10^3 \times L.g^{-1}$)	K_d (ml.g^{-1})	α^{Li}_{Me}
Li^+	16.87	0.019	1.68	99.58	88 421	1
K^+	16.86	15.61	0.124	7.35	7.95	11122
Na^+	16.91	14.64	0.237	13.93	16.18	5464
Mg^{2+}	16.78	16.53	0.025	1.49	1.51	58556

$T = 303$ K, pH = 10, $V = 10$ ml, $W = 100$ mg and time = 120 h.

$KMnO_4 < (NH_4)_2S_2O_8 < Na_2S_2O_8$. This could be satisfied by the electrochemical reactivity of synthesised powders resulting from different oxidising agents. An increase in the nanostructure MnO_2 electrochemical reactivity in the alkaline medium leads to an increase in ionic uptake capacity. Since the ion sieve synthesised by $Na_2S_2O_8$ is more reactive than the ion sieves synthesised by the other oxidizing reagents, the uptake capacity increased in these samples [29]. In fact, the difference in the MnO_2 electrochemical reactivity leads to the difference in the ion exchange capacity, because of the variety of the structure and morphology, the variety of generated impurity, and the number and dimensions of the MnO_2 narrow sized tunnel [29]. Therefore, MnO_2 with higher reactivity has a greater ion exchange capacity.

3.3. Distribution coefficient measurements: Table 9 shows the Li^+ selectivity of the HMO ion sieve compared with the uptake behaviours of other coexisting ions in the enriched solution, including Na^+, K^+ and Mg^{2+}, respectively. The equilibrium distribution coefficients (K_d) of the ion sieve are in the order of $Mg^{2+} < K^+ < Na^+ << Li^+$, indicating high selectivity for lithium ions. Also, there exist more obvious discriminations among the values of the distribution coefficients (K_d) and the separation factor (α^{Li}_{Me}). The relatively high selectivity for Li^+ can be explained by the ion-sieve effect of the spinel lattice with a three-dimensional (1 × 3) tunnel suitable in size for fixing Li^+ in the cubic phase MnO_2 ion sieves obtained from Li–Mn–O precursors. So, Li^+ can enter the (1 × 3) tunnel during the sorption process, while other metal ions can only adsorb on the adsorbent surface sites because of their large ionic radius being too large [15]. The results also indicate that Na^+, K^+ and Mg^{2+} in solution do not interfere with Li^+ during the adsorption/ion-exchange process, since the high concentration factor (C_F) of Li^+ is observed compared with the (C_F) values of other metal ions.

3.4. XRD results: The XRD patterns of the ternary oxide precursor (LMO) and the MnO_2 ion sieve (HMO_{Final}) are given in Fig. 5. The LMO sample could be readily indexed to the pure cubic phase $Li_{1.353}Mn_{1.626}O_4$ [space group: Fd3 m(227), JCPDS 1-088-1087] with the lattice constant $a = 8.148$ Å. The more compact Mn–O lattice made the $Li_{1.353}Mn_{1.626}O_4$ spinel more stable after the Li^+ was extracted. The HMO sample could be indexed to the pure cubic phase $Li_{0.04}Mn_2O_4$ [space group: Fd3 m (227), JCPDS 1-088-0590] with the lattice constant $a = 8.058$ Å calculated according to the equation of $1/d^2 = (h^2 + k^2 + l^2)/a^2$. It should be noted that the XRD patterns of the LMO precursor and the HMO ion sieve were quite similar, assembling the same cubic phase with lattice constants of 8.148 and 8.058 Å, respectively, this indicates that the Mn–O lattice is stable during the Li^+ extraction process and the locations of manganese in the crystal structure are well maintained. The rigid structure with little swelling or shrinking in an aqueous environment is important for the strong

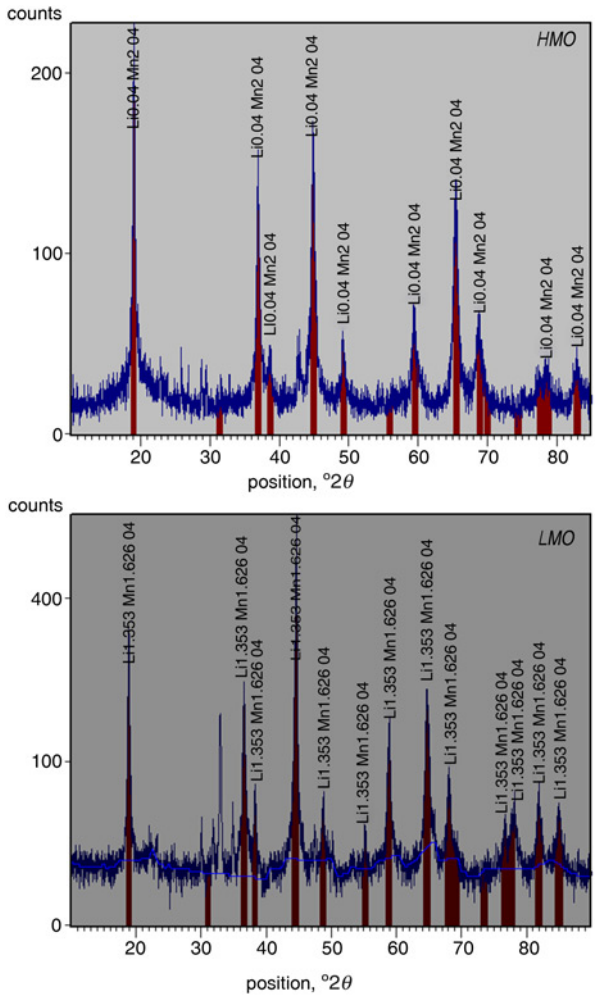

Figure 5 *XRD pattern of LMO precursor and HMO ion-sieve*

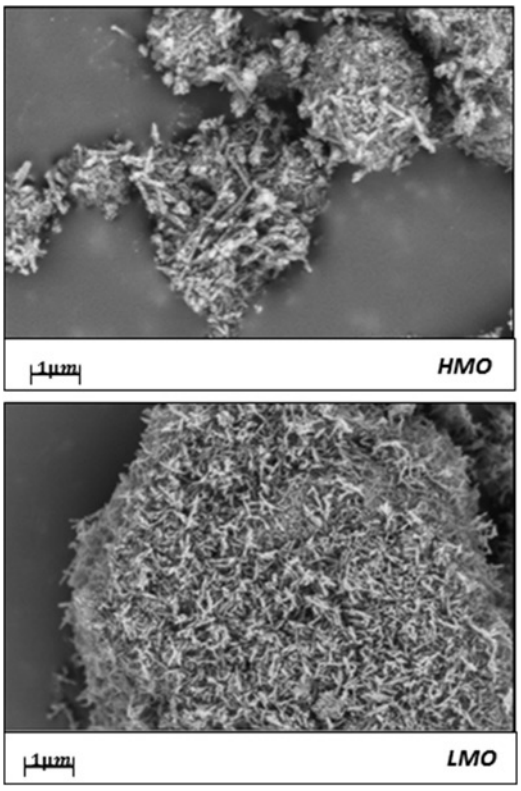

Figure 6 *SEM image of LMO precursor and HMO ion-sieve*

© The Institution of Engineering and Technology 2015

doi: 10.1049/mnl.2014.0342

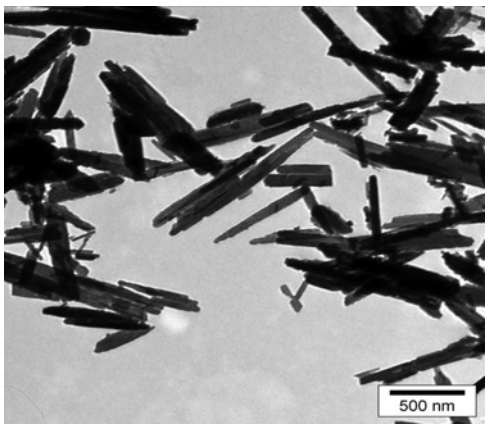

Figure 7 *TEM image of MnO_2 ion-sieve*

steric or the ion-sieve effect of MnO_2 during the lithium selective adsorption process [14].

3.5. SEM and TEM results: In Fig. 6, SEM pictures of the LMO precursor and HMO ion sieve are presented. The results show that all morphologies are the same. The prepared powders show a nanorod morphology of the needle-like structure with sharp edges and rough surfaces. In Fig. 7, the TEM picture reveals that the tiny sticks of the MnO_2 ion sieve, previously characterised by the SEM technique, consist of the assembling of straight needles with diameters less than 50 nm, and lengths up to several hundred nanometres.

However, the high uptake rate and capacity can be related to the special particle structure of the ion sieve, especially the smaller size in length. So, lithium ions can enter the pores from the medium solution and cover the nanorod particles, and because of the ion sieve's special structure, the path way between Li^+ and H^+ ions during the ion exchange process becomes shorter. Therefore, the ion exchange process can be performed easily.

4. Conclusion: A novel manganese oxide was synthesised as a lithium ion sieve using the hydrothermal method. The Taguchi method with the $L_9(3^4)$ orthogonal array was implemented to optimise the experimental conditions for the increasing lithium uptake capacity of synthesised ion sieves. To this end, six parameters including manganese salt compound, lithium salt compound, (Li/Mn) mole ratio, oxidising reagent, calcination temperature and heating time were chosen as the main parameters. As a result, it can be concluded that the lithium salt compound and the oxidising reagent had the most significant effect on lithium adsorption. The best ion sieve with a maximum uptake capacity of more than 9 mmol g^{-1} was synthesised by the explained method for the first time. Compared with past optimised results the lithium uptake capacity increased 35%. So, the presented material is the most promising adsorbent for lithium in sea water because of its large uptake capacity.

5 References

[1] Hunter J.C.: 'Preparation of a new crystal form of manganese dioxide: λ-MnO_2', *J. Solid State Chem.*, 1981, **39**, pp. 142–147

[2] Miyai Y., Ooi K., Katoh S.: 'Recovery of lithium from seawater using a new type of ion-sieve adsorbent based on $MgMn_2O_4$', *Separation Sci. Technol.*, 1988, **23**, (1–3), pp. 179–191

[3] Ammundsen B., Aitchison P.B., Burns G.R., Jones D.J., Rozière J.: 'Proton insertion and lithium-proton exchange in spinel lithium manganates', *Solid State Ion.*, 1997, **97**, (1–4), pp. 269–276

[4] Wang L., Meng C.G., Ma W.: 'Study on Li^+ uptake by lithium ion-sieve via the pH technique', *Colloid Surf. A*, 2009, **334**, (1–3), pp. 34–39

[5] Yang X.J., Tang W.P., Ooi K.: 'Synthesis of $Li_{1.33}Mn_{1.67}O_4$ spinels with different morphologies and their ion adsorptivities after delithiation', *J. Mater. Chem.*, 2000, **10**, pp. 1903–1909

[6] Swierczek K., Marzec M., Molenda J.: 'Crystallographic and electronic properties of $Li_{1+\delta}Mn_{2-\delta}O_4$ spinels prepared by HT synthesis', *Solid State Ion.*, 2003, **157**, pp. 89–93

[7] Shi X., Zhou D., Zhang Z., *ET AL.*: 'Synthesis and properties of $Li_{1.6}Mn_{1.6}O_4$ and its adsorption application', *Hydrometallurgy*, 2011, **110**, (1–4), pp. 99–106

[8] Kaneko S.: 'Adsorption of lithium in sea water on alumina-magnesia mixed-oxide gels', *Colloids Surf. A, Physicochem. Eng. Aspects*, 1990, **47**, pp. 69–79

[9] Chitrakar R., Kanoh H., Makita Y., Miyai Y., Ooi K.: 'Synthesis of spinel-type lithium antimony manganese oxides and their Li extraction/ion insertion reactions', *J. Mater. Chem.*, 2000, **10**, (10), pp. 2325–2329

[10] Chitrakar R., Kanoh H., Ooi K.: 'A new type of manganese oxide ($MnO_2{\cdot}0.5H_2O$) derived from $Li_{1.6}Mn_{1.6}O_4$ and its lithium ion-sieve properties', *Chem. Mater.*, 2000, **12**, (10), pp. 3151–3157

[11] Chitrakar R., Kanoh H., Miyai Y., Ooi K.: 'Recovery of lithium from seawater using manganese oxide adsorbent ($H_{1.6}Mn_{1.6}O_4$) derived from $Li_{1.6}Mn_{1.6}O_4$', *Ind. Eng. Chem. Res.*, 2001, **40**, (9), pp. 2054–2058

[12] Lei J., Chen Y., Gong Q., Sun Y., Zhao J., Yuan Q.: 'Preparation of λ-MnO_2 by column method and is ion-sieve property', *J. Wuhan Univ. Technol. Mater. Sci. Ed.*, 2002, **17**, (4), pp. 9–12

[13] Wang L., Ma W., Liu R., Li H.Y., Meng C.G.: 'Correlation between Li^+ adsorption capacity and the preparation conditions of spinel lithium manganese precursor', *Solid State Ion.*, 2006, **177**, (17–18), pp. 1421–1428

[14] Zhang Q.H., Sun S., Li S., Jiang H., Yu J.G.: 'Adsorption of lithium ions on novel nanocrystal MnO_2', *Chem. Eng. Sci.*, 2007, **62**, (18–20), pp. 4869–4874

[15] Zhang Q.H., Li Sh.P., Sun S.Y., Yin X.S., Yu J.G.: 'Lithium selective adsorption on 1-D MnO_2 nanostructure ion-sieve', *Adv. Powder Technol.*, 2009, **20**, (5), pp. 432–437

[16] Wang L., Meng C., Ma W.: 'Preparation of lithium ion-sieve and utilizing in recovery of lithium from seawater', *Front Chem. Eng. Chin.*, 2009, **3**, (1), pp. 65–67

[17] Tian L., Ma W., Han M.: 'Adsorption behavior of Li + onto nano-lithium ion sieve from hybrid magnesium/lithium manganese oxide', *Chem. Eng. J.*, 2010, **156**, (1), pp. 134–140

[18] Zhang Q.H., Li S.P., Sun S.Y., Yin X.S., Yu J.G.: 'Lithium selective adsorption on low-dimensional titania nano ribbons', *Chem. Eng. Sci.*, 2010, **65**, pp. 165–168

[19] Özgür C.: 'Preparation and characterization of $LiMn_2O_4$ ion-sieve with high Li^+ adsorption rate by ultrasonic spray pyrolysis', *Solid State Ion.*, 2010, **181**, (31–32), pp. 1425–1428

[20] Ma L.W., Chen B.Z., Shi X.C., Zhang W., Zhang K.: 'Stability and Li + extraction/adsorption properties of $LiM_xMn_{2-x}O_4$ (M = ;Ni, Al, Ti; $0 \leq x; \leq 1$) in aqueous solution', *Colloid Surf. A*, 2010, **369**, (1–3), pp. 88–94

[21] Sun S.Y., Song X., Zhang Q.H., Yu J.G.: 'Lithium extraction /insertion process on cubic Li-Mn-O precursors with different Li/Mn ratio and morphology', *Adsorption*, 2011, **17**, (5), pp. 881–887

[22] Roy R.K.: 'Design of experiments using the Taguchi approach: 16 steps to product and process improvement' (Wiley-Interscience, 2001)

[23] Taguchi G., Yokoyama Y.: 'Taguchi methods: design of experiments' (ASI Press, 1993)

[24] Mohammadi T., Moheb A., Sadrzadeh M., Razmi A.: 'Separation of copper ions by electrodialysis using Taguchi experimental design', *Desalination*, 2004, **169**, (1), pp. 21–31

[25] Chou C.S., Yang R.Y., Chen J.H., Chou S.W.: 'The optimum conditions for preparing the lead-free piezoelectric ceramic of $Bi_{0.5}Na_{0.5}TiO_3$ using the Taguchi method', *Powder Technol.*, 2010, **199**, (3), pp. 264–71

[26] Liu W.L., Hsieh Sh., Chen W.J., Lee Jh.: 'Study of nanosized zinc oxide on Cu–Zn alloy substrate using Taguchi method', *Surf. Coat Technol.*, 2007, **201**, (22–23), pp. 9238–9242

[27] Tofighy M.A., Mohammadi T.: 'Salty water desalination using carbon nanotube sheets', *Desalination*, 2010, **258**, (1), pp. 182–186

[28] Norouzbeigi R., Edrissi M.: 'Modification and optimization of nanocrystalline Al_2O_3 combustion synthesis using Taguchi L16 array', *Mater. Res. Bull.*, 2011, **46**, (10), pp. 1615–1624

[29] Benhaddad L., Makhloufi L., Messaoudi B., Rahmouni K., Takenouti H.: 'Reactivity of nanostructured MnO_2 in alkaline medium studied with a microcavity electrode: effect of oxidizing agent', *J. Mater. Sci. Technol.*, 2011, **27**, (7), pp. 585–593

© The Institution of Engineering and Technology 2015